(1)

DIAGNOSTICS DEVELOPMENT FOR E-BEAM EXCITED AIR CHANNELS

Technical Report No. 2

MICROWAVE CAVITY REFLECTION INTERFEROMETER FOR SINGLE-PULSE TRANSIENT CONDUCTIVITY MEASUREMENTS

April 1987

By: D. J. Eckstrom, M. S. Williams, and J. S. Dickinson

Sponsored by:

DEFENSE ADVANCED RESEARCH PROJECTS AGENCY
1400 Wilson Blvd.
Arlington, VA 22209

Monitored by:

NAVAL SURFACE WEAPONS CENTER
Silver Spring, MD 20910

ARPA Order No. 4395
Contract No. N60921-85-C-0210
Effective Date: 21 June 1985
Expiration Date: 21 February 1988
Principal Investigator: D. J. Eckstrom (415) 859-4398

SRI Project PYU-8849
MP Report No. 87-077

SRI International
333 Ravenswood Avenue
Menlo Park, California 94025-3493
(415) 326-6200
TWX: 910-373-2046
Telex: 334486

Unclassified
SECURITY CLASSIFICATION OF THIS PAGE

ADA206963

REPORT DOCUMENTATION PAGE

1a. REPORT SECURITY CLASSIFICATION Unclassified	1b. RESTRICTIVE MARKINGS N/A
2a. SECURITY CLASSIFICATION AUTHORITY DARPA - CG - 55	3. DISTRIBUTION/AVAILABILITY OF REPORT Approved for Public release; distribution unlimited.
2b. DECLASSIFICATION/DOWNGRADING SCHEDULE N/A	
4. PERFORMING ORGANIZATION REPORT NUMBER(S) MP 87-077	5. MONITORING ORGANIZATION REPORT NUMBER(S)
6a. NAME OF PERFORMING ORGANIZATION SRI International 6b. OFFICE SYMBOL (If applicable)	7a. NAME OF MONITORING ORGANIZATION Naval Surface Weapons Center
6c. ADDRESS (City, State, and ZIP Code) 333 Ravenswood Avenue Menlo Park, CA 94025	7b. ADDRESS (City, State, and ZIP Code) Silver Springs, MD 20910
8a. NAME OF FUNDING/SPONSORING ORGANIZATION Defense Advanced Research Projects Agency 8b. OFFICE SYMBOL (If applicable)	9. PROCUREMENT INSTRUMENT IDENTIFICATION NUMBER Contract No. N60921-85-C-0210
8c. ADDRESS (City, State, and ZIP Code) 1400 Wilson Boulevard Arlington, VA. 22209	10. SOURCE OF FUNDING NUMBERS PROGRAM ELEMENT NO: 4395/54 | PROJECT NO | TASK NO | WORK UNIT ACCESSION NO

11. TITLE (Include Security Classification)
Diagnostic Development for E-Beam Excited Air Channels. Microwave Cavity Reflection Interferometer for Single-Pulse Transient Conductivity Measurements.

12. PERSONAL AUTHOR(S)
D.J. Eckstrom, M.S. Williams, and J.S. Dickinson

13a. TYPE OF REPORT	13b. TIME COVERED	14. DATE OF REPORT (Year, Month, Day)	15. PAGE COUNT
Technical No. 2	FROM _____ TO _____	April, 1987	28

16. SUPPLEMENTARY NOTATION

17. COSATI CODES		
FIELD	GROUP	SUB-GROUP

18. SUBJECT TERMS (Continue on reverse if necessary and identify by block number)
Plasma Diagnostics; microwave techniques; Conductivity measurements; electron beams.

19. ABSTRACT (Continue on reverse if necessary and identify by block number)

We describe a technique for measuring real and imaginary conductivity histories in a single pulse using the microwave cavity perturbation technique. The method can be used even when the perturbations are large, e.g., when the frequency shift is larger than the FWHM of the cavity resonance and/or when the cavity Q changes significantly. We demonstrate the use of the technique to measure laser photoionization yields in a high pressure buffer gas. It will also be particularly useful to measure afterglow conductivity decays for electron beam channels from single-pulse accelerators.

20. DISTRIBUTION/AVAILABILITY OF ABSTRACT ☒ UNCLASSIFIED/UNLIMITED ☐ SAME AS RPT. ☐ DTIC USERS	21. ABSTRACT SECURITY CLASSIFICATION Unclassified
22a. NAME OF RESPONSIBLE INDIVIDUAL B.M. Hui	22b. TELEPHONE (Include Area Code) (202) 394-1264 | 22c. OFFICE SYMBOL N60921

DD FORM 1473, 84 MAR 83 APR edition may be used until exhausted. All other editions are obsolete.

SECURITY CLASSIFICATION OF THIS PAGE
Unclassified

CONTENTS

I INTRODUCTION.....1
II CONCLUSIONS.....3
REFERENCES.....4

APPENDIX: Microwave Cavity Reflection Interferometer for Single-Pulse Transient Conductivity Measurements.....A-1

I INTRODUCTION

We have developed the microwave cavity perturbation technique and have used it extensively for two applications important to the development of charged particle beam propagation studies. The first application is to measure the decay of conductivity in the afterglow of electron-beam pulses with the objective of determining the time when the conductivity level is optimum for channel tracking by subsequent pulses and of providing a benchmark for comparison of air chemistry codes that predict the variation of conductivity with time in the afterglow. We have performed extensive measurements on channels generated by a Febetron 706 in our laboratory[1-3] and also on the PHERMEX accelerator at Los Alamos[4] and the Medea accelerator at McDonnell-Douglas Research Laboratory.[5] The second application is to measure the conductivity generated by laser photoionization of organic gases either for laser guiding in accelerators or for creation of synthetic conductivity channels in high pressure gases for tracking studies. In the first category, we used the microwave technique in our laboratory to help determine the relevant photoionization cross sections for four organic molecules that were candidates for laser guiding applications,[6] and later we measured the photoelectron density <u>in situ</u> for Los Alamos experiments involving photoionization of benzene for beam guiding in tenuous atmospheres.[7] In the second category, we have performed a detailed study of the photoionization yields for benzene in the presence of high pressure buffer gases.[8,9]

In all these measurements, use of the microwave technique required generation of numerous repetitive pulses, ranging from a minimum of 40 shots at each condition for the electron-beam experiments to several hundred pulses for laser-generated plasmas. This requirement is clearly unattractive, especially for single-pulse electron accelerators with low duty cycles. Even for repetitively pulsed lasers, there is a problem because laser energy can vary from pulse to pulse and can degrade over a few hundred pulses.

We have now overcome the requirement for multiple-pulse measurements. We have developed a technique that allows full time-dependent real and imaginary conductivity histories in a single pulse, regardless of the gas pressure, and for conductivities that represent large perturbations to the cavity. This technique is described in detail in the Appendix, which is a paper that has been submitted to the Review of Scientific Instruments.

II CONCLUSIONS

This new single-pulse conductivity measurement technique represents a breakthrough in diagnostics capability for charged-particle-beam studies. For single-pulse, low-duty-rate accelerators such as RADLAC, it makes possible accurate afterglow conductivity measurements for the first time. For slightly higher rep-rate accelerators such as Medea or PHERMEX, it will improve the accuracy of the results by eliminating pulse-to-pulse reproducibility problems and will facilitate measurements by substantially reducing the time required. Even for a high rep-rate accelerator such as ATA, advantages are expected in both accuracy and convenience.

The new technique is also very important in synthetic channel characterization. For example, the planned ATA channel tracking studies require determination of the photoelectron densities at several positions, several benzene pressures, and several buffer gas pressures. Acquiring the complete set of data using a multiple-pulse measurement technique and a low-repetition-rate laser would be very difficult if not impossible, but the task is feasible using this new single-pulse technique.

REFERENCES

1. D. J. Eckstrom, "Diagnostics Development for E-Beam Excited Air Channels Conductivity Measurements in Air Afterglows," Technical Report No. 2, Contract N00014-81-C-0208, SRI International (March 1983).

2. M. N. Spencer, J. S. Dickinson, and D. J. Eckstrom, "Diagnostics Development for E-Beam-Excited Air Channels. Afterglow Conductivity Studies of the Febetron Electron Beam," Technical Report No. 1, Contract N00014-84-C-0718, SRI International (July 1985).

3. M. N. Spencer, J. S. Dickinson, and D. J. Eckstrom, "Afterglow Conductivity Measurements of Air and N_2 Following Intense Electron-Beam Excitation," J. Phys. D, Appl. Phys. (to be published).

4. D. J. Eckstrom, J. S. Dickinson, and M. N. Spencer, "Diagnostics Development for E-Beam Excited Air Channels. Conductivity Measurements on the PHERMEX Electron Beam," Technical Report No. 2, Contract N00014-84-C-0718, SRI International (July 1985).

5. M. N. Spencer, J. S. Dickinson, and D. J. Eckstrom, "Diagnostics Development for E-Beam Excited Air Channels. Conductivity Measurements on the Medea Electron Beam," Technical Report No. 3, Contract N00014-84-C-0718, SRI International (September 1985).

6. W. K. Bischel, L. E. Jusinski, M. N. Spencer, and D. J. Eckstrom, "Diagnostics Development for E-Beam Excited Air Channels. Multiphoton Ionization Cross Sections for Selected Organic Molecules at 248 nm," Technical Report No. 5, Contract N00014-84-C-0718, SRI International (February 1985).

7. R. L. Carlson, S. W. Downey, and D. C. Moir, J. Appl. Phys. 61, 12 (1987).

8. D. J. Eckstrom and J. S. Dickinson, "Synthetic Conductivity Channel Formation in High Pressure Air by Benzene Photoionization," presented at the 1986 DARPA Propagation Review, Sandia National Laboratory, Albuquerque, NM (June 1986).

9. D. J. Eckstrom, J. S. Dickinson, and M. S. Williams, Papers CA-8 and CA-9, 39th Gaseous Electronics Conference, Madison, Wisconsin, October 1986 (to be published).

Appendix

MICROWAVE CAVITY REFLECTION INTERFEROMETER FOR SINGLE-PULSE TRANSIENT CONDUCTIVITY MEASUREMENTS

D. J. Eckstrom, M. S. Williams, and J. S. Dickinson
SRI International
Menlo Park, California 94025

Submitted to

Review of Scientific Instruments

MICROWAVE CAVITY REFLECTION INTERFEROMETER FOR SINGLE PULSE TRANSIENT CONDUCTIVITY MEASUREMENTS

D.J. Eckstrom, M.S. Williams, and J.S. Dickinson*
SRI International
Menlo Park, California 94025

ABSTRACT

We describe a technique for measuring transient real and imaginary conductivity histories in a single pulse using the microwve cavity perturbation technique when the perturbations are large, that is, when the ferquency shift is larger than the FWHM of the cavity resonance and/or when the cavity Q changes significantly. A demonstration of the use of the technique to measure laser photoionization yields in a high pressure buffer gas is presented.

* Current address: Portland State University, Portland, Oregon 97207

INTRODUCTION

Microwave cavity techniques have frequently been used to measure the conductivities of plasmas. These techniques are based on the cavity perturbation formula derived by Slater[1]

$$\Delta\left(\frac{1}{Q}\right) - 2j\,\frac{\Delta f}{f} = \frac{1}{\epsilon_o\,\omega}\,\frac{\int_v(\sigma_r + j\sigma_i)\,E^2(v)dv}{\int_v E^2(v)dv} \qquad (1)$$

This relation shows that the change in Q of the cavity resonance varies with the real conductivity of the plasma, whereas the shift of the resonance frequency varies with the imaginary conductivity. The conductivities can be written in the constant-collision frequency approximation (ν = constant) as

$$\sigma_r = \epsilon_o\omega_p{}^2\nu/(\omega^2 + \nu^2) \qquad (2)$$

and

$$\sigma_i = \epsilon_o\omega_p{}^2\omega/(\omega^2 + \nu^2) \qquad (3)$$

Thus, both conductivities vary linearly with the electron density, but at higher pressures the conductivities also depend strongly on the electron collision frequency. At high gas pressures the cavity perturbation tends to be dominated by the Q change, whereas at low pressures it is dominated by the frequency shift. At intermediate pressures, it is necessary to measure both the frequency shift and the Q change to determine either the real or the imaginary conductivity. Because of this difficulty, measurements are often confined to low pressures where Q changes are negligible or to very small plasma perturbations where the Q changes can again be neglected. However, it is then possible to measure only one of the conductivities (usually the imaginary component) and so the electron density can be calculated only if the

collision frequency is assumed known. We address here the case where it is necessary to measure both components of the conductivity.

The most straightforward way to measure the Q and f_o of the cavity is to sweep the microwave source across the resonance and measure either the transmitted or the reflected power versus frequency. For a steady-state or slowly varying plasma, this measurement can be repeated to determine the perturbed Q and f_o', and the perturbations $\Delta(1/Q)$ and Δf are easily determined. However, when the plasma density and/or temperature vary rapidly, swept-frequency measurements are no longer possible, and alternative techniques are required. One approach that we have used extensively[2] is to measure transmission histories at many frequencies across the cavity resonance, each measurement being made on a separate transient plasma decay. We then crossplot the transmission values at discrete times in the afterglow versus frequency, thus reconstructing instantaneous transmission curves that allow determination of the perturbation at each time. However, this technique requires many repetitive pulses of the plasma, which may not always be possible; furthermore, the plasma may not be reproducible from shot to shot.

The shift of cavity resonance frequency is analogous to a phase change in a transmission experiment, whereas the Q change is analogous to attenuation. In microwave interferometer measurements, the attenuation and phase shift are easily determined and interpreted, and transient conductivity decays can be determined for a single pulse. However, there are cases in which a single-pass measurement using an interferometer may not be sensitive enough, and the enhancement achieved by the "multiple" interaction of the standing waves in the cavity with the plasma may be desired. Furthermore, it is very difficult to measure plasmas of small dimensions comparable to the microwave wavelength by single-pass interferometry because of refraction effects on the beam,

whereas such measurements present no difficulty using the cavity technique. If the transient change in transmission or reflection and the change in phase of the transmitted or reflected power for a cavity could be simultaneously measured and if those changes could be interpreted in terms of $\Delta(1/Q)$ and Δf, then transient real and imaginary conductivities could be measured in a single pulse. We describe the method for accomplishing such measurements in the next section.

I. REFLECTIONS FROM A MICROWAVE CAVITY

Pound[3] showed that the power reflected from a microwave cavity changes phase as the incident frequency varies around the resonant frequency of a cavity and used that fact to design a feedback scheme to stabilize microwave oscillators. His derivation forms the basis for the present scheme, and our description and notation will follow his presentation. Fessenden and Warman,[4] Shimamori and Hatano,[5] and others also developed diagnostic methods based on Pound's work, but they restricted their measurements to small perturbations (Δf smaller than the half-width of the resonance) and assumed that the amplitude of the reflected signal stayed constant (thus precluding measurement of the real conductivity component).

In electrical circuit terms, the cavity can be represented by a resistance R, an inductance L, and a capacitance C; in the shunt-resonant representation, the three components are connected in parallel across the input terminals of the equivalent circuit. The cavity admittance is then given by the expression[6]

$$Y_c = (R/Z_o^2) + j\, R(\omega C - 1/\omega L)/Z_o \qquad (4)$$

where Z_o is the characteristic impedance of the transmission line. In Pound's notation, this is written

$$Y_c/Y_o = (\delta_o/\delta_1) + j\ (2\Delta\nu/\delta_1) \tag{5}$$

where $\delta_o = 1/Q_u$, $\delta_1 = 1/Q_{ext} = 1/Q_\ell - 1/Q_u$, $\Delta\nu = (\nu - \nu_o)/\nu_o$, and $Y_o = 1/Z_o$. Q_u, Q_ℓ, and Q_{ext} are the unloaded, loaded, and external Q's, respectively, and ν_o is the cavity resonant frequency, $\nu_o = 1/2\pi(LC)^{1/2}$.

The <u>voltage</u> reflection coefficient for the cavity is[6]

$$\Gamma_V = (Y_o - Y_c)/(Y_o + Y_c) \tag{6}$$

Again using Pound's notation where $\alpha = \delta_o/\delta_1$ and $a = 2\Delta\nu/\delta_o$, this is

$$\Gamma_V = \frac{1 - \alpha - j\,\alpha a}{1 + \alpha + j\,\alpha a}$$

$$= \frac{(1 - \alpha^2 - \alpha^2 a^2) - j\,2\alpha a}{(1 + \alpha)^2 + \alpha^2 a^2} \tag{7}$$

This relationship is fundamental to our analysis. It shows that the voltage reflection coefficient varies with the Q of the cavity through the parameter α and with the frequency offset through the parameter a.

Equation (7) shows that the voltage reflection coefficient is complex, so that it could alternately be written as an amplitude and a phase angle ϕ

$$\Gamma_V = |\Gamma_V| \angle \phi \tag{8}$$

The amplitude is always ≤ 1, and the imaginary component is zero when $a = 0$ or when $a \to \pm\infty$. In the latter case, the real component is -1; that is, the phase angle is 180° when the frequency is far from resonance (thus, the cavity acts like a short circuit). Likewise, at resonance the phase angle is either 0 or 180° depending on whether the real component is positive or negative. Positive values correspond to an overcoupled cavity ($\alpha < 1$), whereas negative values correspond to undercoupling ($\alpha > 1$). When the cavity is matched, the reflection at resonance is zero. As the frequency approaches resonance from below, the phase angle decreases to values smaller than 180°, and at frequencies above resonance, the angle is between 0 and -180°.

The variation of the reflection coefficient with frequency can be seen more readily by means of a Smith chart, as shown in Fig. 1. It can be shown[6] that the locus of points representing the complex reflection coefficient for a given Q and f_o is a circle centered on the negative real axis at the point ρ_o, where

$$\rho_o = -\alpha/(1 + \alpha) \tag{9}$$

and with a radius $\rho = 1 + \rho_o$, or

$$\rho = 1/(1 + \alpha) \tag{10}$$

As the frequency is increased from 0, the reflection coefficient traverses the circle in a clockwise fashion beginning at -1. At resonance, $a = 0$, and the reflection coefficient is at the second intersection of the circle with the axis. As frequencies continue to increase above resonance, the coefficient continues to traverse the circle in the lower half plane back to -1. Since the phase angle is that angle between the positive x axis and points on the circle, its variation with frequency is clearly apparent.

II. INTERPRETATION OF EXPERIMENTS

In the next section, we describe techniques for determining the time-dependent magnitudes and phase angles of the voltage reflection coefficient through measurement of the power reflection coefficient, Γ_p, and the interference power. The power reflection coefficient is the square of the amplitude of the voltage reflection coefficient

$$\Gamma_p = |\Gamma_V|^2 \tag{11}$$

The two voltage coefficient parameters suffice to define a point (x,y) in the complex reflection plane as

$$x = \Gamma_p^{1/2} \cos \phi \tag{12}$$

$$y = \Gamma_p^{1/2} \sin \phi$$

This point lies on the circle representing all possible reflection coefficients for the value of α of the cavity (i.e., for its Q_u and Q_{ext}). Identification of the radius, ρ, of the circle allows determination by means of Eq. (10) of the instantaneous value of α (which gives the instantaneous value of Q_ℓ), while identification of the angular position of the point on that circle (say, as the angle θ) allows specification of the parameter a (and hence, the frequency offset $\Delta\nu$).

Trigonometric calculations lead to the result that the radius ρ is given by

$$\rho = \frac{[\, y^2 + (x + 1)^2]}{2(x + 1)} \tag{13}$$

which, with equation (10), gives

$$\alpha = \frac{2(x + 1)}{[y^2 + (x + 1)^2]} - 1 \qquad (14)$$

It can also be shown that the angle $\theta/2$ as shown on Fig. 1 is

$$\tan (\theta/2) = y/(x + 1) = - \alpha a/(1 + \alpha) \qquad (15)$$

This leads to

$$a = - \frac{2\ y}{2(x + 1) - y^2 - (x + 1)^2} \qquad (16)$$

Equations (14) and (16) allow the determination of the parameters α and a at each instant that the phase and magnitude of reflected power can be measured.

The presence of a plasma in the cavity can be regarded as perturbing the unloaded Q_u while the external Q_{ext} stays constant. Then

$$\Delta(1/Q) = \Delta(\delta_o) = \delta_1 \Delta\alpha = \delta_1 (\alpha - \alpha^o) \qquad (17)$$

where the superscript indicates the value for the empty (unperturbed) cavity. The frequency shift is given by

$$\Delta f/f = \Delta(\Delta\nu) = (a\alpha - a^o\alpha^o)\delta_1/2 \qquad (18)$$

The perturbations given by Eqs.(17) and (18) are used directly in equation (1) to calculate the real and imaginary conductivities.

The parameters δ_1 and α^o can be determined by sweeping the source across the empty cavity and measuring Δf_{FWHM}, the frequency spread at the half-power points, and the reflection coefficient at resonance, $\Gamma_p{}^o$. After using Eq. (7)

to find an expression for Γ_p and then setting a = 0 in that expression, one can show that

$$\alpha^o = [(1 - \Gamma_p{}^{o\ 1/2})/(1 + \Gamma_p{}^{o\ 1/2})]^{\pm 1} \qquad (19)$$

Also,

$$\delta_1 = 1/Q_{ext} = 1/[(1 + \alpha^o)\ Q_\ell{}^o]$$

$$= \Delta f_{FWHM}/[(1 + \alpha^o)\ f_{res}] \qquad (20)$$

where $f_{res} = \nu_o$ is the cavity resonance frequency. The superscript +1 is used in Eq. (19) if the cavity is overcoupled, and -1 is used if undercoupled (see also Section V).

The parameter a^o is calculated for the "operating frequency" f_{op} as

$$a^o = 2(f_{op} - f_{res})/(f_{res}\ \delta_o{}^o) \qquad (21)$$

where

$$\delta_o{}^o = \alpha^o\ \delta_1 \qquad (22)$$

For maximum sensitivity, the measurement would be performed with f_{op} at the frequency corresponding to the half-power point of transmission or reflection, where the slope of reflected power with perturbation is greatest, but the range of electron densities that can be measured can be extended to higher values by setting f_{op} to even higher values.

III. EXPERIMENTAL SETUP

A microwave circuit suitable for measuring magnitude and phase of the reflected power from a cavity is shown in Fig. 2. The setup is essentially the same as for an interferometer, but the horns and open-air propagation path

are replaced by the cavity and directional coupler #2. Other configurations are possible. For example, directional coupler #2 could be replaced by a circulator, while directional coupler #4 could be replaced by a hybrid junction (magic tee) or a balanced mixer. The setup shown simplifies the interpretation of the results.

If detector D_1 is calibrated for power, then the power reflection coefficient is determined by comparing that power with the value measured off resonance, that is, either by sweeping the microwave source far from resonance or by shifting the resonance far from the empty-cavity value, for example, by inserting a quartz rod into the cavity. This measurement gives one of the fundamental values required, $\Gamma_p(t)$.

Likewise, if detector D_2 is calibrated for power, it gives the value of the interference signal:

$$P_2 = P_A + P_B + 2\,(P_A P_B)^{1/2} \cos(\phi_B - \phi_A) \qquad (23)$$

where A and B refer to the reference arm and the reflected signal arm, respectively. We adjust the variable attenuator so that the powers reaching D_2 are approximately equal when the frequency is far from resonance. Likewise, we adjust the variable phase shifter so that the two signals are approximately in quadrature for the same condition. Since $\phi_B = 180^\circ$ in that case, this specifies $\phi_A = 90^\circ$. Note that the quadrature adjustment could also give $\phi_A = 270^\circ$; the correct choice gives a maximum in P_2 as the frequency approaches resonance from below and a minimum at frequencies above resonance.

Once we have chosen f_{op}, we can calculate the corresponding phase angle from Eq. (7) as

$$\phi_{op} = \tan^{-1}\{(-2\ \alpha^{o}\ a_{op})/[1 - (\alpha^{o})^{2} - (\alpha^{o}a_{op})^{2}]\} \qquad (24)$$

Then, by measuring P_A, P_B, and P_2 at that operating frequency, we can determine ϕ_A exactly from Eq. (23) using the measured powers and $\phi_B = \phi_{op}$.

Having determined P_A and ϕ_A from these preliminary calibrations, we can now make a transient measurement by measuring $P_B(t)$ and $P_2(t)$ using D_1 and D_2. We can then use equation (23) to determine the instantaneous reflected power phase angle as

$$\phi_B(t) = \phi_A + \cos^{-1}\{[P_2(t) - P_A - P_B(t)]/2[P_A P_B(t)]^{1/2}\} \qquad (25)$$

This is the angle used in Eq. (12). Note again that ϕ_A will be near 90^{o} when set as described above.

IV. EXAMPLE OF MEASUREMENT TECHNIQUE

We have performed an extensive set of measurements of the photoionization yields of benzene by a KrF laser when the benzene is admixed in a high pressure buffer gas. We used the microwave cavity perturbation technique with repetitive pulses as described in Reference 2. However, we were ultimately limited by shot-to-shot jitter in the laser energy, which spurred us to develop the single-shot technique reported here.

Details of the measurements and of the photophysics of benzene have been reported elsewhere.[7] Here, we note only that we were using a cavity resonant in the TM_{010} mode at 1.6 GHz and that the combination of benzene pressure and

laser energy used led to a predicted value of electron density of ~1 x 10^{10} cm^{-3} within the 7.3-mm-diameter laser beam path. The loop antenna that couples the cavity to the transmission line was adjusted to produce slight undercoupling for the unperturbed cavity and also for the perturbed cavity at low gas pressures where the Q change is small. At higher gas pressures, the perturbation became progressively stronger, making the transient undercoupling more pronounced.

In Fig. 3, we present Smith-chart representations of the amplitude and phase of the voltage reflection coefficients following laser pulses into 1 μm of benzene and 0, 10, and 100 torr of N_2. When no N_2 is present, the real conductivity is very small and the Q change is negligible. Then the reflection coefficient traces out nearly a perfect circle corresponding to that for the empty cavity (the fluctuations in the curve near the origin occur because calculation of the phase angle involves division by the reflected power, which approaches zero in that region). At the higher pressures, both the amplitude and phase values change to reflect the effects of collisions on the real and imaginary conductivities. In these cases, the reflection coefficient returns toward the empty cavity value as the plasma decays, but the measurements were not continued long enough to reach the unperturbed condition.

The time histories of the conductivities are shown in Figure 4, and those of the electron densities are shown in Figure 5. In the case of no N_2, the electron decay is governed by ambipolar diffusion, and therefore the decay is exponential. For N_2 = 10 and 100 torr, electron-ion recombination dominates, and the decays follow a n_e^{-1} t dependence. As noted above, these and other results of the benzene photoionization study will be reported in detail elsewhere.[7]

V. DETAILS ON IMPLEMENTING THE TECHNIQUE

The general comment can be made that achievement of accurate results using this method requires exceptional precision and accuracy in both the hardware and the measurements. Thus, for example, we found it necessary to insert an isolator between the directional couplers DC_1 and DC_2 (Fig. 2) to prevent reflected power from the cavity from entering the reference leg of the interferometer, even though DC_1 had a nominal directivity of 18 dB. Likewise, the calibrations of the detectors must be accurate to a few percent; note that D_1 should be calibrated in terms of the power appearing at D_2.

Another problem we encountered was that of obtaining a flat reflected power versus frequency in the vicinity of the resonance when the resonance was shifted away. We identified the problem as one of power radiated from the loop antenna even when far from resonance. The problem was worse when the antenna size was large enough to provide near matched coupling to the cavity. We found that it could be eliminated by modifying the antenna as shown in Fig. 6. With this geometry, we obtained near matched coupling and a baseline reflection coefficient flat to 1.2% over a 10-MHz frequency range around 1.6 GHz.

Finally, we found it difficult to determine whether the empty cavity was slightly overcoupled or slightly undercoupled, so as to determine the correct sign of the exponent in Eq. (19). An unambiguous determination can be made by perturbing the cavity by inserting a quartz rod into the cavity a small step at a time. At each position, the reflected and interference powers are measured, and the voltage reflection coefficient and phase angle are calculated, the latter parameter from Eq. (25). The results are then plotted on a Smith chart. Note that the value of α^o is required to calculate ϕ_{op} from Eq. (24); that angle is then used to calculate ϕ_A, which is used to calculate

the ϕ_B's that are plotted. If the wrong sign of the exponent is chosen, so that α^o is incorrect, the plotted points will not form a circle, but will instead be skewed. Repeating the procedure using the reciprocal for α^o should then lead to a good circle and identification of the correct value of α^o.

ACKNOWLEDGMENT

This work was supported by the Defense Advanced Research Projects Agency through Naval Surface Weapons Center Contract N60921-85-C-0210.

1. J. C. Slater, Rev. Modern Phys. 18, 441 (1946).
2. M. N. Spencer, J. S. Dickinson, and D. J. Eckstrom, J. Phys. D, Appl. Phys. (to be published).
3. R. V. Pound, Proc. I.R.E. 35, 1405 (1947).
4. R. W. Fessenden and J. M. Warman, in Radiation Chemistry, Vol II, Advances in Chemistry Series 82 (American Chemical Society, 1968).
5. H. Shimamori and Y. Hatano, Chem. Phys. Lett. 38, 242 (1976).
6. A. F. Harvey, Microwave Engineering (Academic Press, London, 1963).
7. D. J. Eckstrom, J. S. Dickinson, and M. S. Williams, Papers CA-8 and CA-9, 39th Gaseous Electronics Conference, Madison, Wisconsin, October 1986 (to be published).

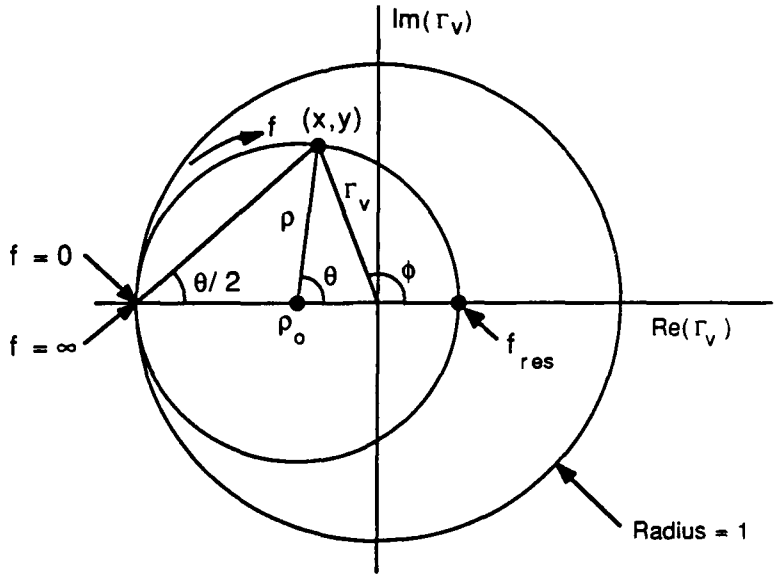

(a) Definitions of parameters

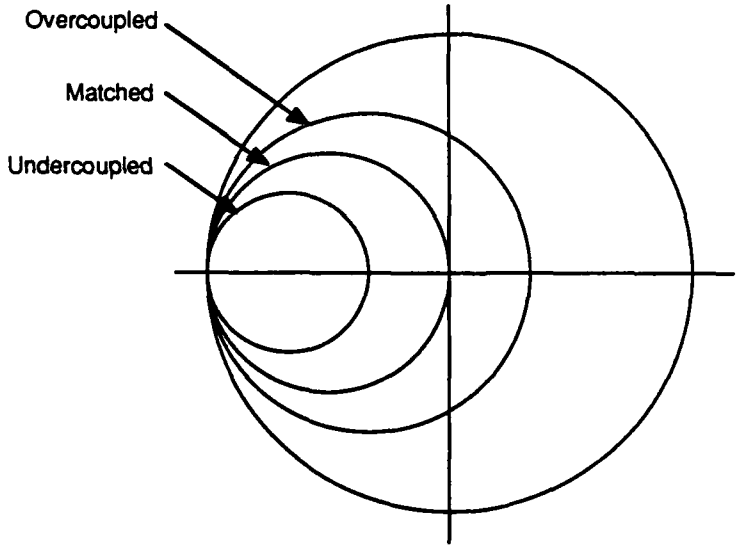

(b) Typical circles representing loci of voltage reflection coefficients

JA-M-8849-136

FIGURE 1 SMITH CHART REPRESENTATION OF COMPLEX VOLTAGE REFLECTION COEFFICIENTS NEAR RESONANCE OF MICROWAVE CAVITY

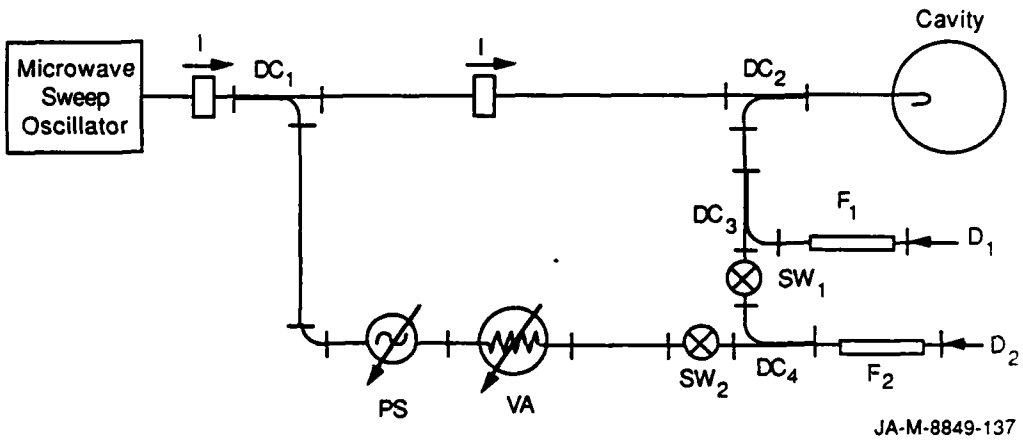

FIGURE 2 EXPERIMENTAL SETUP FOR MICROWAVE CAVITY REFLECTION INTERFEROMETER
I = isolator; DC = directional coupler; PS = phase shifter; VA = variable attenuator; D = detector; SW = switch; F = bandpass filter. SW and F are optional.

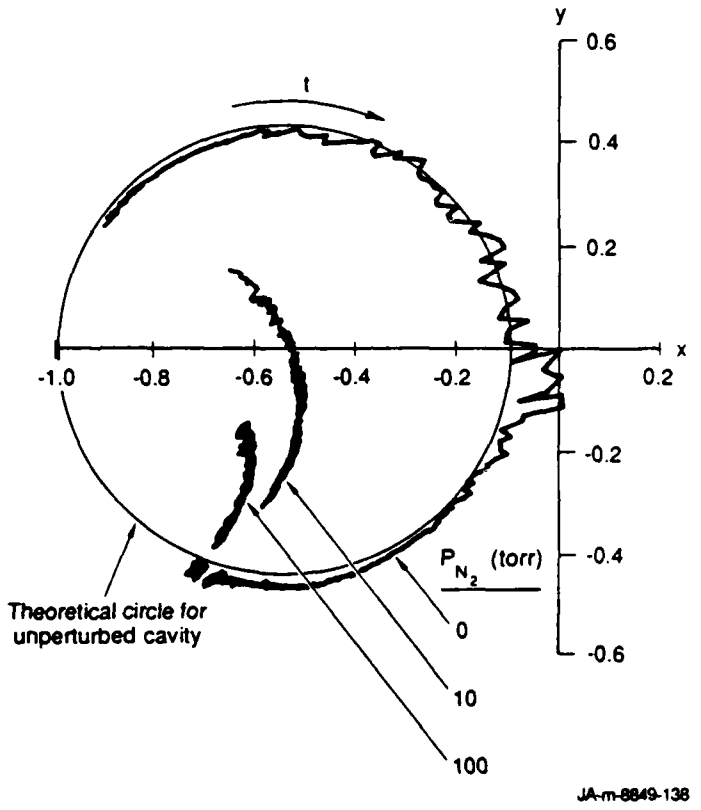

FIGURE 3 LOCI OF REFLECTION COEFFICIENTS FOR CONDUCTIVITY DECAY FOLLOWING PHOTOIONIZATION OF BENZENE IN N_2

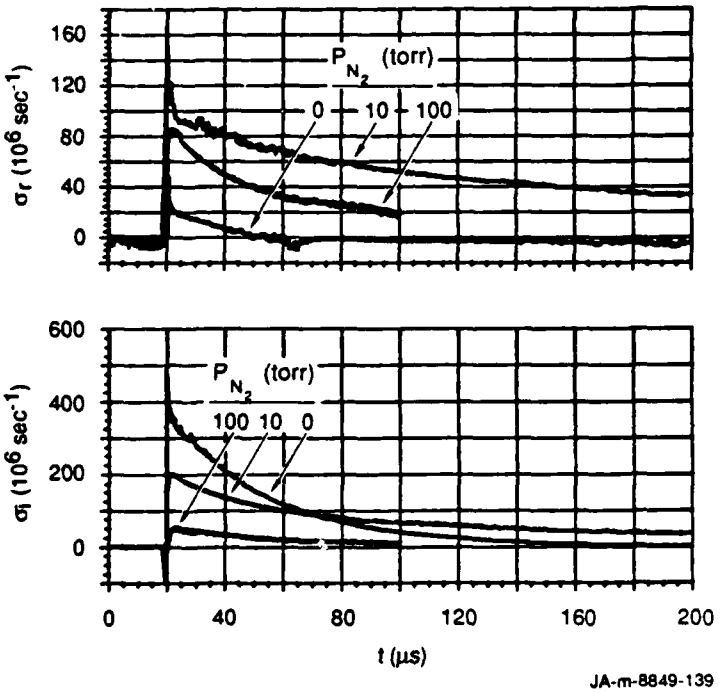

FIGURE 4 REAL AND IMAGINARY CONDUCTIVITY HISTORIES FOLLOWING PHOTOIONIZATION OF BENZENE IN N_2

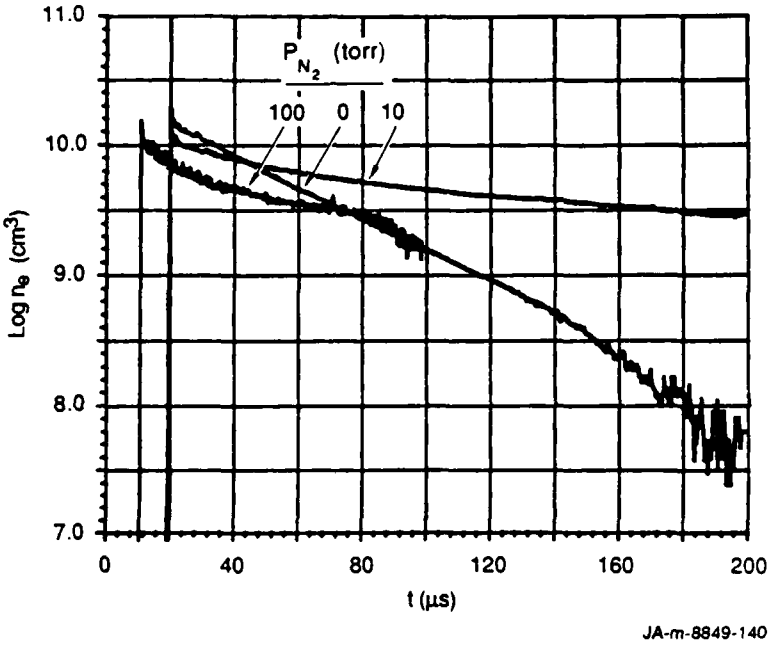

FIGURE 5 ELECTRON DENSITY DECAY HISTORIES FOLLOWING PHOTOIONIZATION OF BENZENE IN N_2

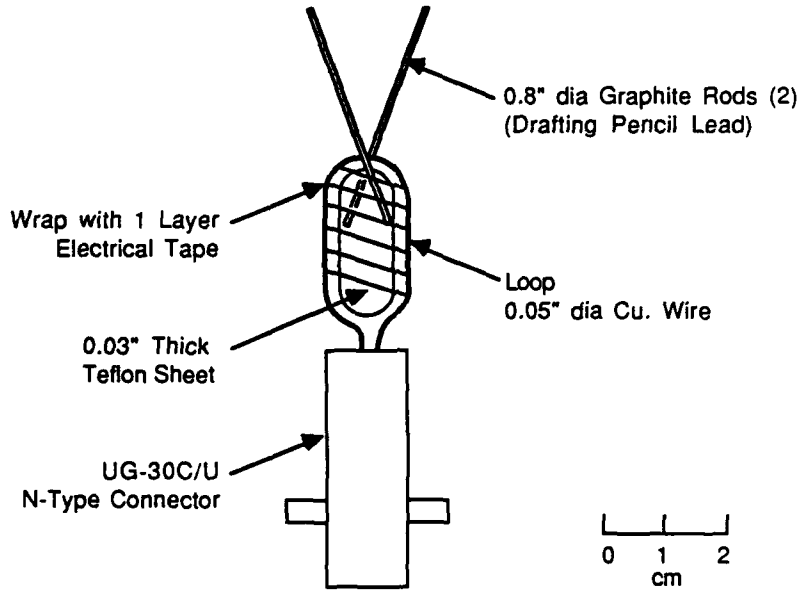

FIGURE 6 SCHEMATIC OF COUPLING LOOP ANTENNA